Supporting Information

V modified Ni-based layer hydroxide for the electrocatalytic upgrading of amines to nitriles

Shaoxiong Bai,[a,b] Liang Chen,*[a] Jingjing Bai,[a] Chenghang Lv,[c] Shoudong Xu,[b] Ding Zhang,[d] Haibin Meng,[a] Chunli Guo,[c] Huimin Yang,*[a] and Chenjing Shang*[e]

a. College of Chemistry, Taiyuan University of Technology, Taiyuan 030024, PR China. Email: chenliang@tyut.edu.cn, yanghuimin@tyut.edu.cn

b. College of Chemical Engineering and Technology, Taiyuan University of Technology, Taiyuan 030024, PR China.

c. College of Materials Science and Engineering, Taiyuan University of Technology, Taiyuan 030024, PR China.

d. School of Chemical Engineering and Pharmacy, Wuhan Institute of Technology, Wuhan 430205, PR China.

e. Shenzhen Key Laboratory of Marine Bioresource and Eco-environmental Science, College of Life Sciences and Oceanography, Shenzhen University, Shenzhen 518060, PR China. E-mail address: cjshang@szu.edu.cn

Experimental Section

Materials and Chemicals.

$NiCl_2 \cdot 6H_2O$, $Ni(NO_3)_2 \cdot 6H_2O$, KOH, NaCl, $Na_2S_2O_4$, and urea were purchased from Sinopharm Chemical Reagent Co., Ltd. NH_4VO_3, $Fe(NO_3)_3 \cdot 9H_2O$, benzylamine, benzonitrile, and ethylacetate were obtained from Aladdin Reagent Co., Ltd. Ethanol and hydrochloric acid (HCl) were purchased from Xilong Chemical Reagent Co. Ltd. Nickel foam was obtained from Changde Liyuan New Material Co. Ltd. All the reagents were of analytical grade and used as received without further purification.

Synthesis of NiV-LDH on nickel foam (NiV-LDH/NF)

The nickel foam (NF) was soaked in 1 M HCl and ultrasonically cleaned for 15 min to remove the oxide layer on the surface. The cleaned NF was ultrasonicated separately with deionized (DI) water and alcohol for 15 min, and then dried in a vacuum oven at 60 °C for 6 h. To prepare solution A, 0.234 g (2 mmol) NH_4VO_3 and 0.292 g NaCl were dissolved in 12 mL DI water. Then, 8 mL of 1 M HCl was added to give an orange solution. After adding 4 mL of 0.5 M $Na_2S_2O_4$, the dark green solution A was obtained. Meanwhile, 0.285 g (1.2 mmol) $NiCl_2 \cdot 6H_2O$ was dissolved in 35.2 mL DI water to form solution B. Solution B, together with 4.8 mL of the as-prepared solution A (containing 0.4 mmol vanadium) and 0.3 g urea, was then transferred to a 50 mL Teflon-lined stainless-steel autoclave. A piece of cleaned NF (2×5 cm^2) was placed in the autoclave which was then sealed and maintained at 120 °C for 12 h. After natural cooling down to room temperature, the as-prepared NiV-LDH/NF was rinsed three times with DI water and ethanol, and then dried in a vacuum oven at 50 °C for 6 h.

Synthesis of $Ni(OH)_2$ on nickel foam ($Ni(OH)_2$/NF)

For comparison, $Ni(OH)_2$/NF was also obtained via a hydrothermal method. Typically, 0.380 g $NiCl_2 \cdot 6H_2O$ and 0.3 g urea were dissolved in 40 mL of DI water and stirred to form a homogeneous solution. Afterwards, the above solution was then transferred to a 50 mL Teflon-lined stainless-steel autoclave. Then, a piece of cleaned Ni foam (2×5 cm^2) was placed in the autoclave which was then sealed and maintained at 120 °C for 12 h. After natural cooling down to room temperature, the as-synthesized

$Ni(OH)_2$/NF was collected and then rinsed three times with DI water and ethanol, and then dried in a vacuum oven at 50 °C for 6 h.

Material characterization

Powder X-ray diffraction (XRD) analysis was performed on a Bruker D8 Advance powder diffractometer with Cu Kα X-ray radiation (λ = 1.5406 A). Scanning electron microscopy (SEM) images were obtained by FEI Talos-S. Transmission electron microscope (TEM) was performed by JEOL JSM-7100F operated at 200 kV. X-ray photoelectron spectroscopy (XPS) spectra were collected on a Thermo ESCALAB 250Xi X-ray photoelectron spectrometer. The shift of the binding energy is corrected using C 1*s* as an internal standard at 284.8 eV. The pH is measured by a PHSJ-5 pH meter (Leici, Co. Ltd., China). The products were analyzed by ^{1}H NMR (Bruker AVANCE III 400M) and GC (Agilent GC 7890A).

Electrochemical measurements

All the electrochemical measurements were carried out on a Corrtest CS3104 electrochemical workstation with a configured three-electrode system, in which graphite rod and Hg/HgO electrode served as the counter electrode and reference electrode, respectively. The as-prepared catalyst was selected as the working electrode. The current density was normalized based on the geometric area of the working electrode (1×1 cm^2). Before the electrochemical measurement, 20 cycles cyclic voltammetry (CV) were conducted at scan rate of 50 mV s^{-1} in the range of 0.1 ~ 0.3 V (*vs*. Hg/HgO) to make the catalyst stabilized. The linear sweep voltammetry (LSV) curves in this report were obtained with 90% iR compensation except specially denoted. The applied potential was calibrated based on the reversible hydrogen electrode (RHE), which was calculated using the formula of *E* (*vs*. RHE) = *E* (*vs*. Hg/HgO) + 0.096 V + 0.059 V × pH. The electrochemical impedance spectroscopy (EIS) measurement was carried out in the frequency range between 0.01 Hz and 100 kHz with an alternating voltage amplitude of 5 mV at various potentials. The electrochemical surface areas (ECSAs) were evaluated from the electrochemical double layer capacitance (C_{dl}) with a potential range from 1.01 ~ 1.21 V *vs*. RHE at the scan rates of 20 ~ 100 mV s^{-1}. For comparison, the OER and BOR performances of prepared catalyst were characterized

under the same conditions. The OER and BOR experiments were conducted in 30 mL of 1 M KOH with and without 3 mmol benzylamine, respectively.

To calculate the activation energy of different catalysts for BOR, the LSV curves of BOR with different electrocatalysts were measured at various temperature controlled by environmental chamber (MJS-E42). The apparent electrochemical activation energy (E_a) for BOR can be determined using the Arrhenius' relationship

$$\left[\frac{\partial(\log i_k)}{\partial(1/T)}\right]_\eta = \frac{E_a}{2.3R}$$

where i_k (mA cm^{-2}) is the kinetic current at 1.5 V *vs*. RHE at different temperatures, T (K) is the temperature, and R is the universal gas constant (8.314 J mol^{-1} K^{-1}). The Arrhenius plots for the different catalysts can be obtained, and E_a can be extracted from the slop.

In situ ATR-FTIR spectroscopy measurements.

FTIR experiments were run on a Thermo Scientific Nicolet 7600 FT-IR spectrometer with attenuated total reflection (ATR) configuration using MCT detector. All spectra were collected at a resolution of 4 cm^{-1} at a bottom-up incidence angle of ca. 60°.The ultrasonic-dispersed catalyst ink was dropped on a glassy carbon electrode as a working electrode (WE). The reference and counter electrodes were Hg/HgO and graphite rod, respectively. The electrolyte was 1 M KOH with 0.1 M benzylamine. The spectra were collected in a 30 min test under an applied potential of 0 to 0.6 V vs. Hg/HgO and was collected at 0.5 V vs. Hg/HgO for 1 hour in the range from 3000 to 1000 cm^{-1}. Before the measurements, the spectrometer and electrolyte were purified with high-purity Ar gas.

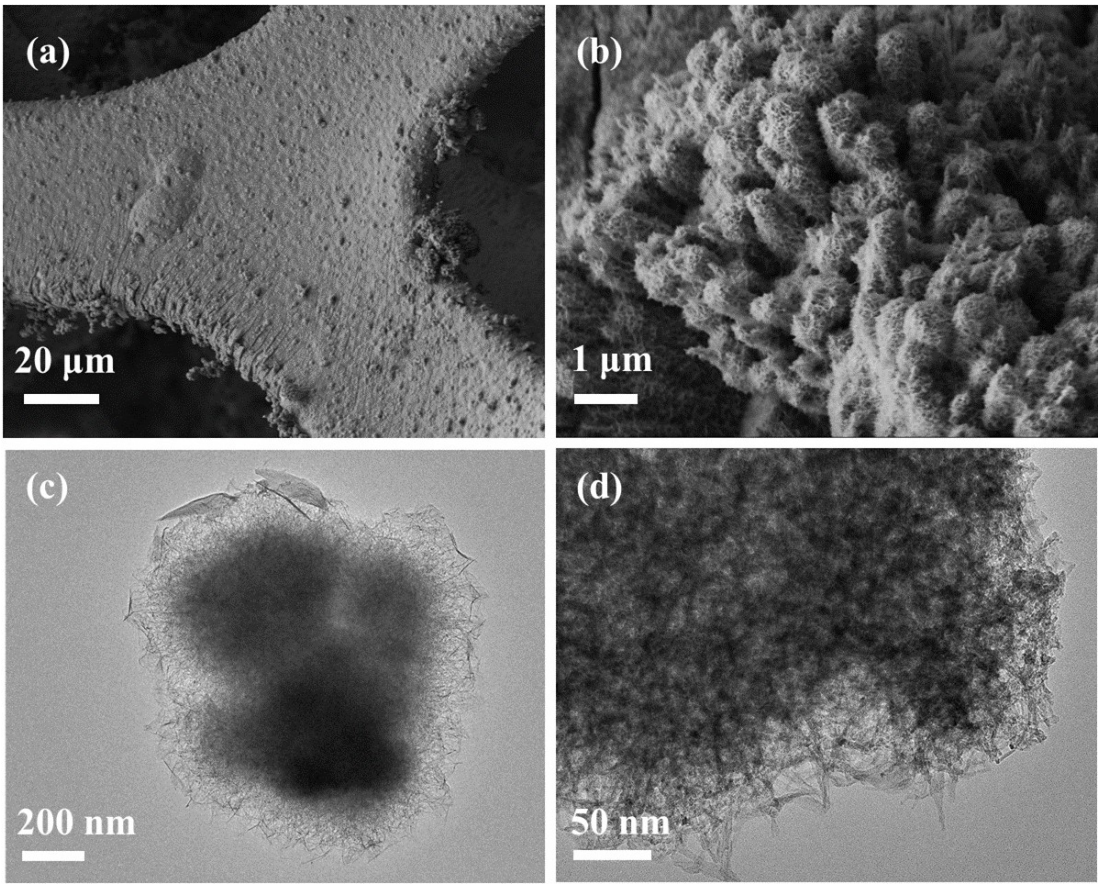

Figure S1. (a, b) SEM and (c, d) TEM images of NiV-LDH/NF.

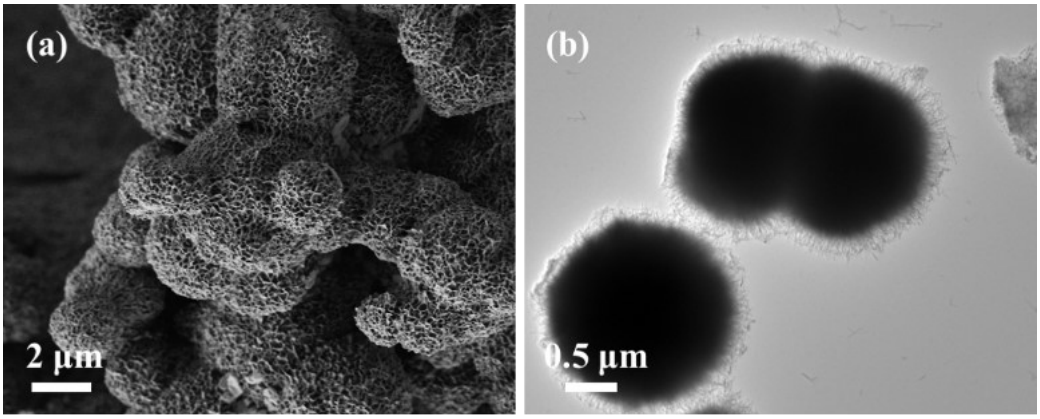

Figure S2. (a) SEM and (c) TEM images of $Ni(OH)_2$/NF.

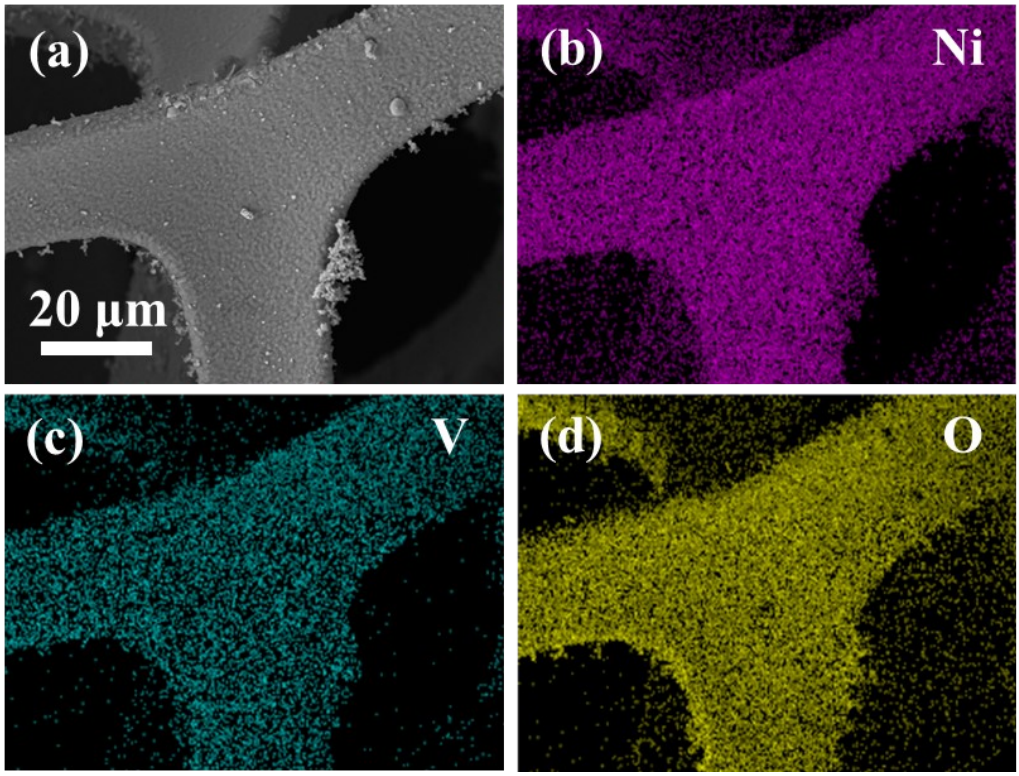

Figure S3. (a) SEM image and (b-d corresponding EDS elemental mapping images of NiV-LDH/NF.

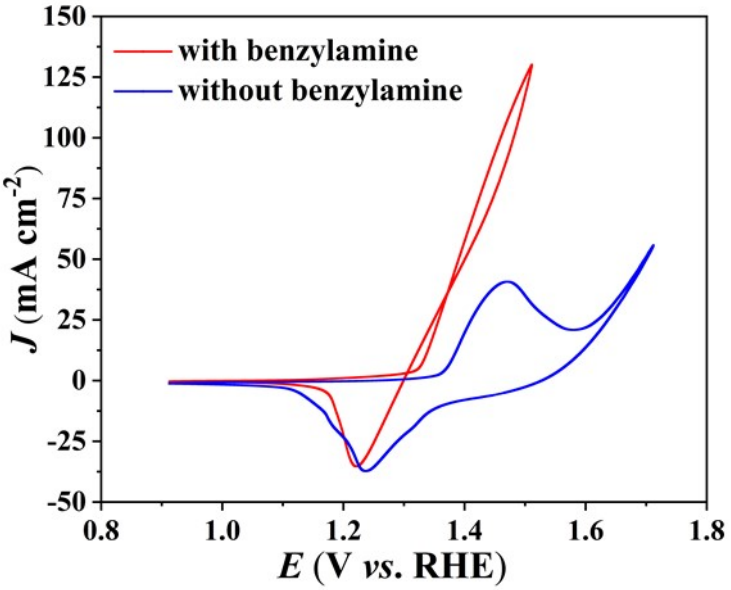

Figure S4. CV curves of the NiV-LDH/NF electrode in 1.0 M KOH with and without benzylamine (the scan rate is 5 mV/s).

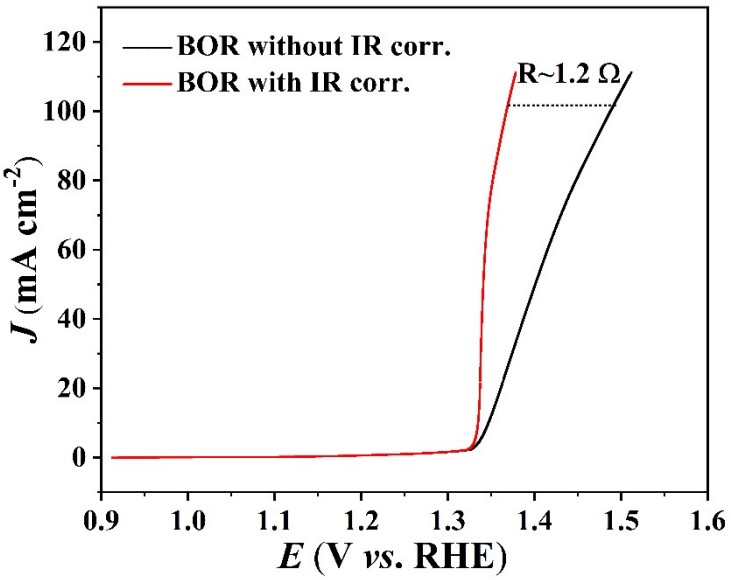

Figure S5. LSV curves of the NiV-LDH/NF for BOR with and without iR correction.

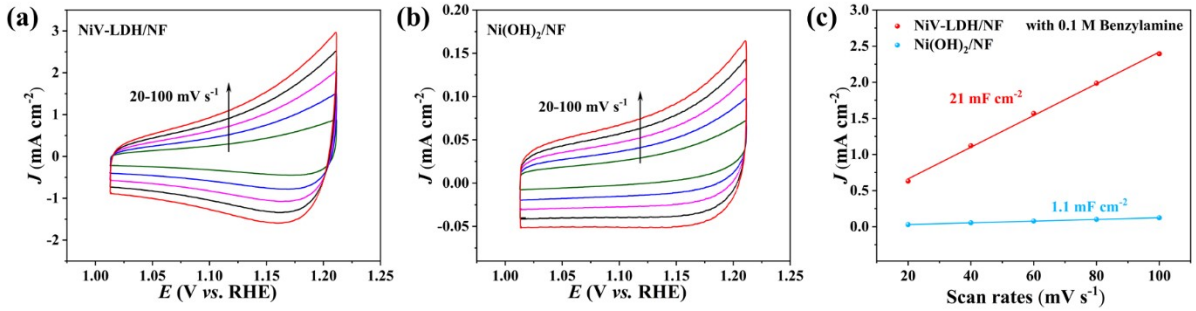

Figure S6. CV curves of (a) NiV-LDH/NF and (b) $Ni(OH)_2$/NF in the non-Faraday region. (c) Electrical double-layer capacitance ($C_{(dl)}$) for the corresponding samples.

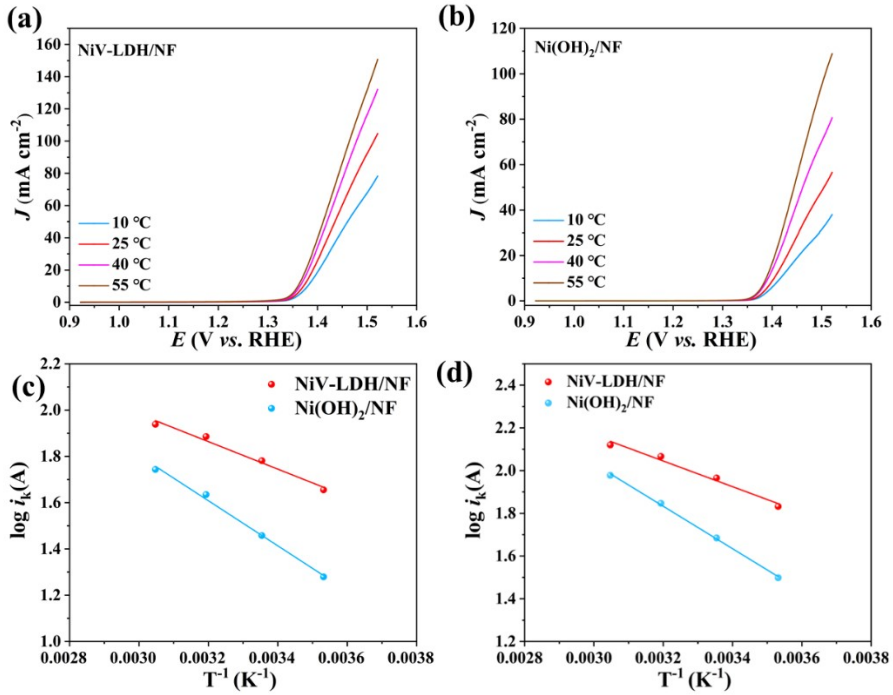

Figure S7. LSV curves of the (a) NiV-LDH/NF and (b) $Ni(OH)_2$/NF electrodes at different temperatures. Arrhenius plots of the NiV-LDH/NF and $Ni(OH)_2$/NF electrodes at (c) 1.45 V *vs*. RHE and (d) 1.5 V *vs.* RHE.

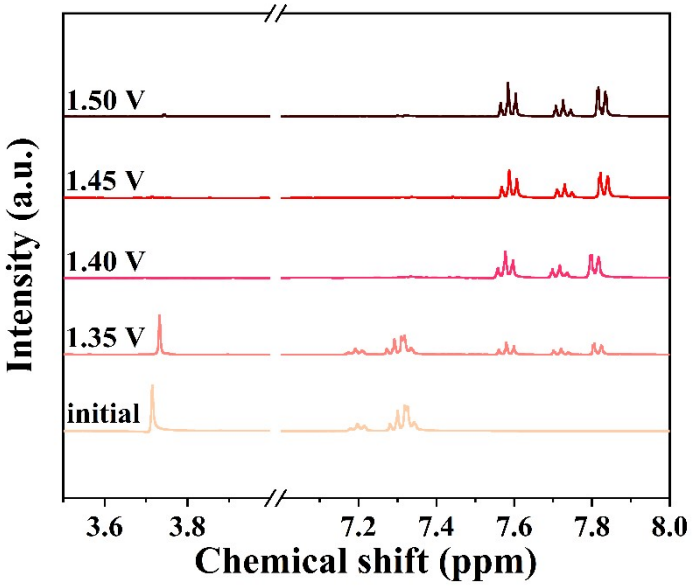

Figure S8. ^1H NMR of electrolyte catalyzed by NiV-LDH/NF at different potentials.

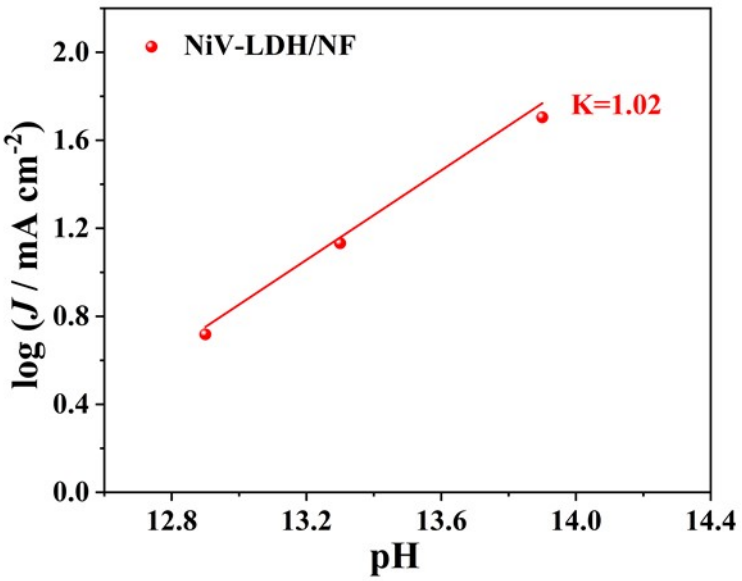

Figure S9. The dependence of the BOR current density on the pH of the electrolyte at 1.4 V vs. RHE.

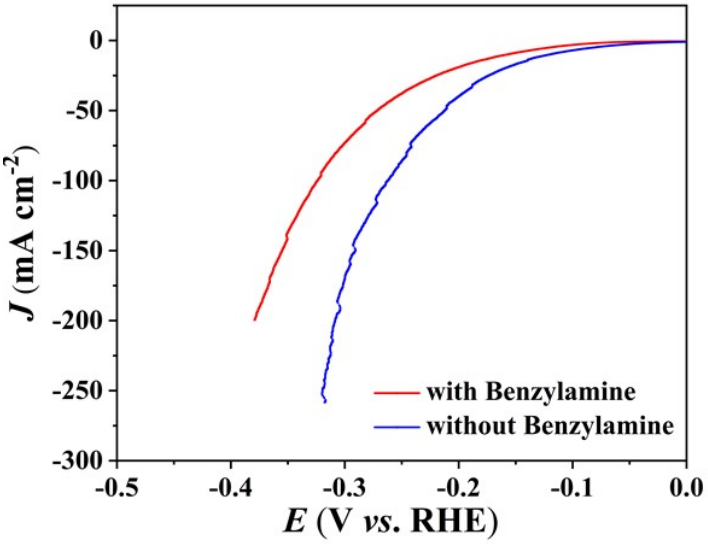

Figure S10. The LSV curves for the HER of NiV-LDH/NF in 1 M KOH electrolyte with and without 0.1 M benzylamine (with 80% iR correction)

Table S1. Electrocatalytic benzylamine oxidation performance for other reported catalyst.

Catalysts	Electrolyte	Potential (V *vs.* RHE)	Ref.
		10 mA cm^{-2}	
NiV-LDH	1 M KOH 0.1 M benzylamine	1.33	This work
NiSe	1 M KOH 0.001 M benzylamine	1.34	1
$NiFeO_x$	1 M NaOH 0.2 M benzylamine	1.39	2
Ni_3N	1 M KOH 2 mmol benzylamine	1.35	3
Mn-doped Ni $(OH)_2$	1 M KOH 0.025 M benzylamine	1.39	4
$CoSe_2$/Ni−SVs	1 M KOH 0.02 M benzylamine	1.34	5
Ni@C/NiNCNT	1 M KOH 0.04 M benzylamine	1.34	6
Ni_2P-UNMs	1M KOH 25 mmol benzylamine	1.34	7

1 Y. Huang, X. Chong, C. Liu, Y. Liang and B. Zhang, Boosting Hydrogen Production by Anodic Oxidation of Primary Amines over a NiSe Nanorod Electrode, *Angew. Chem., Int. Ed.*, 2018, **57**, 13163-13166.

2 B. Mondal, N. Karjule, C. Singh, R. Shimoni, M. Volokh, I. Hod and M. Shalom, Unraveling the Mechanisms of Electrocatalytic Oxygenation and Dehydrogenation of Organic Molecules to Value-Added Chemicals Over a Ni–Fe Oxide Catalyst, *Adv. Energy Mater.*, 2021, **11**, 2101858.

3 F. Ma, S. Wang, L. Han, Y. Guo, Z. Wang, P. Wang, Y. Liu, H. Cheng, Y. Dai, Z. Zheng and B. Huang, Targeted Regulation of the Electronic States of Nickel Toward the Efficient Electrosynthesis of Benzonitrile and Hydrogen Production, *ACS Appl. Mater. Interfaces*, 2021, **13**, 56140-56150.

4 H. Sun, C. W. Tung, Y. Qiu, W. Zhang, Q. Wang, Z. Li, J. Tang, H. C. Chen, C. Wang and H. M. Chen, Atomic Metal-Support Interaction Enables Reconstruction-Free Dual-Site Electrocatalyst, *J Am Chem Soc*, 2022, **144**, 1174-1186.

5 L. Zeng, W. Chen, Q. Zhang, S. Xu, W. Zhang, F. Lv, Q. Huang, S. Wang, K. Yin, M. Li, Y. Yang, L. Gu and S. Guo, CoSe2 Subnanometer Belts with Se Vacancies and Ni Substitutions for the Efficient Electrosynthesis of High-Value-Added Nitriles Coupled with Hydrogen Generation, *ACS Catal*, 2022, **12**, 11391.

6 X. Cao, Y. Wang, D. Tan, B. Wulan, J. Ma, W. Guo and J. Zhang, Stepwise dispersion of nickel species for efficient coupling of electrocatalytic redox reactions, *Chem. Eng. J*, 2023, **454**, 140062.

7 Y. Ding, B.-Q. Miao, S.-N. Li, Y.-C. Jiang, Y.-Y. Liu, H.-C. Yao and Y. Chen, Benzylamine oxidation boosted electrochemical water-splitting: Hydrogen and benzonitrile co-production at ultra-thin Ni_2P nanomeshes grown on nickel foam, *Appl. Catal. B Environl*, 2020, **268**, 118393.